CrystEngComm

Accepted Manuscript

ROYAL SOCIETY OF CHEMISTRY

www.rsc.org/crystengcomm

CrystEngComm

PAPER

N-donor ligands enhancing luminescence properties of seven Zn/Cd (II) MOFs based on a large rigid π-conjugated carboxylate ligand

Received 00th January 20xx,
Accepted 00th January 20xx

DOI: 10.1039/x0xx00000x

www.rsc.org/

Run-Ping Ye,[ab] Xin Zhang,[a] Ji-Quan Zhai,[a] Ye-Yan Qin,[a] Lei Zhang,[a] Yuan-Gen Yao[*a] and Jian Zhang[a]

A series of Zn/Cd (II) coordination polymers, namely $[Zn(IDPA)(H_2O)]_n{\cdot}n(H_2O)$ **(1)** $[Cd(IDPA)(bpp)]_n{\cdot}n(H_2O)$ **(2)**, $[Cd(IDPA)(4,4'\text{-}bpy)_{1/2}]_n$ **(3)**, $[Zn(IDPA)(4,4'\text{-}bpy)_{1/2}]_n$ **(4)**, $[Zn_4(IDPA)_4(phen)_2{\cdot}(H_2O)_2]_n{\cdot}2n(H_2O)$ **(5)**, $[Zn(IDPA)(phen){\cdot}(H_2O)]_n{\cdot}n(H_2O)$ **(6)** and $[Zn(IDPA)(2,2'\text{-}bpy){\cdot}(H_2O)]_n{\cdot}n(H_2O)$ **(7)**, have been prepared on the basis of a bulky 1,3-benzenedicarboxylate derivative ligand, 5-(1-oxoisoindolin-2-yl) isophthalic acid (H_2IDPA), with the help of 1,3-bis(4-pyridyl)propane (bpp), 4,4'-bipyridine (4,4'-bpy), 1,10-phenanthroline (phen) or 2,2'-bipyridine (2,2'-bpy) as secondary ligands. H_2IDPA is a luminous ligand with a large rigid π-conjugated system, and the solid-state luminescence properties of compounds **1-7** have been comparatively investigated. The results indicate that their luminescence properties have been enhanced compared to free ligand, especially for the compounds **2-7** which have been further regulated by N-donor ligands with π-conjugated system. Compound **2** is a 2D layer structure and its quantum yield (QY) is 39.80%, which is much higher than the QY of H_2IDPA ligand (QY=4.41%) and compound **1** (QY=6.32%). From the viewpoint of crystal structure diversity and comparison, our results further demonstrate that ligands with large π-conjugated system has a promotional effect on luminescence properties of coordination polymers.

Introduction

The design and synthesis of metal-organic frameworks (MOFs) have attracted great attention not only due to their properties as potential materials for gas storage, ion exchange, chemical separations, nonlinear optics, and heterogeneous catalysis, but also owing to their intriguing structure and diverse topologies.[1-2] In particular, considerable efforts have been dedicated to complexes based on d^{10} metals because of their attractive luminescence functionality and potential applications in light-emitting diodes.[3] However, fluorescence is often weakened or quenched at high concentrations or in solid states, a phenomenon widely known as “aggregation-caused quenching”.[4] Recently, an opposite mechanism, namely, aggregation-induced emission (AIE) has been identified and studied to turn on the fluorescence by building the fluorophore within MOFs.[5] Generally, the luminescence properties of coordination polymers (CPs) could be rationally enhanced by tuning many subtle factors such as temperature,[6] rare-earth metal ions[7] and solvent system.[7a, 8] Herein we employ a strategy for improving the room-temperature luminescence properties of Zn/Cd (II) complexes based on a rigidified ligand with the help of several N-donor auxiliary ligands.

To the best of our knowledge, aromatic compounds exist luminescence properties due to their conjugation effect and π to π^* or n orbital transitions.[3d, 9] Ligands with large π-conjugated system would be used to improve the luminescence properties.[10] However, most of the reported work has been devoted to the use of simple rigid aromatic carboxylic acids, such as 1,3-benzenedicarboxylic acid (1,3-BDC),[11] 1,3,5-benzenetricarboxylic acid (1,3,5-BTC)[1d, 12] and 1,2,4,5-benzenetetracarboxylic acid (1,2,4,5-BTEC)[13] and their derivative ligands have been rarely investigated. Considering these in mind, we have introduced a versatile novel ligand, 5-(1-oxoisoindolin-2-yl) isophthalic acid (H_2IDPA), to construct unprecedented metal complexes. The new 1,3-BDC derivative ligand has a large rigid π-conjugated system in which aromatic substituent is coplanar with the benzene ring, with the aim of enhancing and stabilizing delocalization in the ligand of the potentially luminescent ligand-to-ligand charge-transfer (LLCT) state and decreasing the energy gap. In addition, the H_2IDPA ligand exhibits several other interesting characters: (i) five potential coordination sites of two carboxyl groups and one oxygen group, which can provide varied coordinating patterns in the construction of fascinating coordination frameworks. (ii) the 5-position of 1,3-BDC is replaced by a bulky idl (isoindolin-1-one) substituent group, which can twist or bend the plane of the benzene ring and therefore facilitate supramolecular isomerism through conformational diversity. (iii) the oxygen atom of idl group could act as hydrogen-bond acceptor as well as neighboring C-H acting as hydrogen-bond donor, which further constructs a intra hydrogen bond network. Furthermore, because of

---

[a] *Key Laboratory of Coal to Ethylene Glycol and Its Related Technology, Fujian Institute of Research on the Structure of Matter, Chinese Academy of Sciences, Fuzhou, Fujian 350002, China. E-mail: yyg@fjirsm.ac.cn; Fax: +86-591-8371-4946; Tel: +86-591-63173138*
[b] *University of Chinese Academy of Sciences, Beijing, 100049, China.*

† Footnotes relating to the title and/or authors should appear here. Electronic Supplementary Information (ESI) available: See DOI: 10.1039/x0xx00000x

the strong coordination affinity and capability of d^{10} metal centers, it is effective to introduce auxiliary ligands in preparing metal carboxylate CPs with enhanced luminescence properties.[14] Herein, we further fabricate CPs with various common pyridine and phenanthroline ligands because of their excellent π-conjugated system and the relatively simple coordination geometries of the nitrogen atoms.[15] In addition, an analysis of the Cambridge Structural Database (CSD) reveals that this ligand has never been studied, only reporting some analogous benzenedicarboxylate derivative ligands such as 2,3-naphthalenedicarboxylic acid, 5-(N-phthalimide)isophthalic acid and 4-(1,3-dioxo-1,3-dihydro-isoindol-2-yl)-benzoicacid.[16]

Considering all the above-mentioned aspects, we have introduced two d^{10} metal ions (Zn/Cd^{II}) and two kinds of pre-designed building blocks in this work: (1) H$_2$IDPA—as the primary ligand, taking advantage of its versatile coordination ability and the luminous property; (2) four different N-donor ligands—as reliable linkers for the construction of CPs with improved luminescence properties (Scheme 1).[16c, d] Therefore, three 1D chain CPs $[Zn(IDPA)(H_2O)]_n \cdot n(H_2O)$ **(1)**, $[Zn(IDPA)(phen)\cdot(H_2O)]_n \cdot n(H_2O)$ **(6)** and $[Zn(IDPA)(2,2'\text{-bpy})\cdot(H_2O)]_n \cdot n(H_2O)$ **(7)**, two 2D layer CPs $[Cd(IDPA)(bpp)]_n \cdot n(H_2O)$ **(2)** and $[Zn_4(IDPA)_4(phen)_2\cdot(H_2O)_2]_n \cdot 2n(H_2O)$ **(5)**, two 3D CPs $[Cd(IDPA)(4,4'\text{-bpy})_{1/2}]_n$ **(3)** and $[Zn(IDPA)(4,4'\text{-bpy})_{1/2}]_n$ **(4)** have been successfully synthesized under solvothermal methods. In addition, their thermal stabilities and slightly different luminescence properties have been systematically investigated in the solid state at room temperature.

<void space for Scheme 1>

Experimental section

Materials and Methods

All the reagents and solvents employed in the present work were obtained from commercial sources and used directly without further purification. All compounds were synthesized under an autogenous pressure with 20 mL glass vials. Elemental analyses (C, H, and N) were performed on an EA1110 CHNS-0 CE elemental analyzer. The FT-IR spectra were recorded from KBr pellets in the range 4000-400 cm^{-1} with a Nicolet Magna 750 FT-IR. The powder X-ray diffraction (PXRD) data were collected on a Rigaku Dmax2500 diffractometer with Cu-Kα radiation (λ= 1.54056 Å) with a scan speed of 5°/min. TG data were collected at a heating rate of 10 K/min on a NETSCHZ STA-449C thermal analyzer in the temperature range 30–990 °C under nitrogen atmosphere. The luminescence spectra were measured at 293 K with a HITACHI F-4600 luminescence spectrophotometer. The quantum yield (QY) measurements were performed on FLS920 produced by EDINGBURGH INSRUMENTS by means of an integrating sphere. The absolute error on the quantum yield values is about ±1%. The decay time were performed on FLS980 produced by EDINGBURGH INSRUMENTS.

Synthesis of $[Zn(IDPA)(H_2O)]_n \cdot n(H_2O)$ (1).

The starting materials of $Zn(NO_3)_2 \cdot 6H_2O$ (0.0297g, 0.1mmol), H$_2$IDPA (0.0297g, 0.1mmol), DMF (1mL) and H$_2$O (2mL) were sealed in a 20 mL capped *via*l. The pH value was adjusted to 9.5 with 0.5mol/L NaHCO$_3$ solution, then the resulting mixture was heated at 90℃ for two days. After a slow cooling to room temperature, colorless piece-shaped crystals suitable for X-ray diffraction analysis were separated by filtration with the yield of 0.0246g, 62% (based on H$_2$IDPA ligand). Anal. calcd for $C_{16}H_{13}ZnNO_7$ (396.66): C 48.40, H 3.28, N 3.53. Found: C 48.56, H 3.22, N 3.59. IR/cm^{-1} (KBr): 3694 (w), 1705 (m), 1534 (s), 1361 (s), 1078 (m), 924 (m), 773 (m), 732 (m).

Synthesis of $[Cd(IDPA)(bpp)]_n \cdot n(H_2O)$ (2).

$Cd(NO_3)_2 \cdot 4H_2O$ (0.0246g, 0.1mmol), H$_2$IDPA (0.0297g, 0.1mmol) and bpp (0.0198g, 0.1mmol) were dissolved in 3mL of DMF/ H$_2$O (2:1, v/v), and a drop of concentrated H$_2$NO$_3$ was added to adjust the pH of the reaction system to 5.5, and then the solution was placed in a 20 mL glass vial. The mixture was heated at 90°C for two days and then cooled to room temperature. Colorless block crystals of the product were formed and collected by filtration and then washed with DMF several times (yield: 52% based on H$_2$IDPA). Anal. Calcd. for $C_{29}H_{25}CdN_3O_6$: C 55.78, H 4.01, 6.73. Found: C 55.86, H 4.19, N 6.64. IR/cm^{-1} (KBr): 3517(m), 2927(w), 1684(s), 1619(s), 1564(s), 1367(s), 1218(m), 810(m), 776(s), 726(s).

Synthesis of $[Cd(IDPA)(4,4'\text{-bpy})_{1/2}]_n$ (3).

Compound **3** was prepared similarly to **2**, except that bpp (0.0198g, 0.1mmol) was replaced by 4,4'-bpy (0.0156g, 0.1mmol). Colorless block crystals of **3** were formed and collected by filtration and then washed with DMF several times (yield: 47% based on H$_2$IDPA). Anal. Calcd. for $C_{21}H_{13}CdN_2O_5$: C 51.88, H 2.68, N 5.76. Found: C 51.34, H 2.76, N 5.71. IR/cm^{-1} (KBr): 3448(s), 2920(w), 1593(s), 1345(s), 1218(m), 805(m), 769(m), 719(w).

Synthesis of $[Zn(IDPA)(4,4'\text{-bpy})_{1/2}]_n$ (4).

Compound **4** was prepared similarly to **3**, except that $Cd(NO_3)_2 \cdot 4H_2O$ (0.0246g, 0.1mmol) was replaced by $Zn(OAc)_2 \cdot 2H_2O$ (0.0219g, 0.1mmol). Colorless block crystals of **4** were formed and collected by filtration and then washed with DMF several times (yield: 43% based on H$_2$IDPA). Anal. Calcd. for $C_{21}H_{13}ZnN_2O_5$: C 57.44, H 2.96, N 6.38. Found: C 57.52, H 2.89, N 6.32. IR/cm^{-1} (KBr): 3440(s), 2927(w), 1676(s), 1612(s), 1388(s), 1218(m), 1072(m), 817(m), 776(s), 726(s).

Synthesis of $[Zn_4(IDPA)_4(phen)_2\cdot(H_2O)_2]_n \cdot 2n(H_2O)$ (5).

$Zn(NO_3)_2 \cdot 6H_2O$ (0.0297 g, 0.1 mmol) H$_2$IDPA (0.0297g, 0.1mmol), and phen (0.018g, 0.1mmol) were dissolved in 3mL of DMF/ H$_2$O (2:1, v/v), and several drops of ethanol were added to adjust the pH value to 7.5, and then the solution was placed in a 20 mL glass vial. The mixture was heated at 90°C for three days and then cooled to room temperature. Colorless block crystals of the product were formed and collected by filtration and then washed with DMF several times (yield: 58% based on H$_2$IDPA). Anal. Calcd. for $C_{88}H_{60}Zn_4N_8O_{24}$: C 56.32, H 3.20, N 5.97. Found: C 56.38, H 3.31, N 5.89. IR/cm^{-1} (KBr): 3426(w), 3076(w), 1676(s), 1612(m), 1564(s), 1388(s), 1093(m), 813(m), 784(s), 733(s).

Synthesis of $[Zn(IDPA)(phen)\cdot(H_2O)]_n\cdot n(H_2O)$ (6).

Compound **6** was prepared similarly to **5**, except that the volume ratio of DMF/ H_2O (2:1) was changed to 1:2 and the pH value was adjusted to 11.0 with 0.5mol/L NaOH solution. Colorless block crystals of **6** were formed and collected by filtration and then washed with DMF several times (yield: 69% based on H_2IDPA). Anal. Calcd. for $C_{28}H_{21}ZnN_3O_7$: C 58.25, H 3.64, N 7.28. Found: C 58.33, H 3.69, N 7.35. IR/cm^{-1} (KBr): 3539(m), 3068(w), 1698(s), 1619(s), 1571(s), 1367(s), 1108(m), 853(m), 784(s), 726(m).

Synthesis of $[Zn(IDPA)(2,2'\text{-bpy})\cdot(H_2O)]_n\cdot n(H_2O)$ (7).

Compound **7** was prepared similarly to **6**, except that phen (0.018g, 0.1mmol) was replaced by 2,2'-bpy (0.0156g, o.1mmol). Colorless block crystals of **7** were formed and collected by filtration and then washed with DMF several times (yield: 63% based on H_2IDPA). Anal. Calcd. for $C_{26}H_{21}N_3ZnO_7$: C 56.43, H 3.80, N 7.60. Found: C 56.51, H 3.85, N 7.67. IR/cm^{-1} (KBr): 3524(m), 3083(w), 1684(s), 1612(m), 1578(s), 1360(s), 810(w), 776(s), 726(m).

Single Crystal X-ray Diffraction Determination

Data were collected on a computer-controlled Oxford Xcalibur E diffractometer with graphite monochromatic Mo-Kα radiation ($\lambda_{Mo\text{-}K\alpha}$ = 0.71073 Å) at 298K. Final unit cell parameters were derived by global refinements of reflections obtained from integration of all the frame data. Empirical absorption corrections were applied using the SADABS program. The structures were solved by the direct method and refined by full-matrix least-squares (*SHELXL-97*) on F^2 with the *SHELXS-97* program.[17] Anisotropic thermal parameters were used for the non-hydrogen atoms and isotropic parameters for the hydrogen atoms. Hydrogen atoms were added geometrically and refined using a riding model. 'AFIX' command was used to restrain the benzene ring in complex **5**. The crystal data and other pertinent information of **1–7** are summarized in Table 1. Selected bond lengths and bond angles with their estimated standard deviation are listed in Table S1 (ESI†). CCDC 1417805 and 1419208-1419213 for complexes **1-7**, respectively, contain the supplementary crystallographic data for this paper.

<void space for Table 1>

Results and discussion

Synthesis of the Complexes 1−7

As shown in Scheme 1, one dicarboxylate ligand was chosen and used to assemble complexes with the help of N-donor ligands including bpp, 4,4'-bpy, phen and 2,2'-bpy. In the present study, complexes **1−7** were prepared based on the solvothermal reaction between the H_2IDPA ligand and corresponding transition metals together with N-donor secondary ligands in a molar ratio of 1:1:1. The reaction between H_2IDPA ligand and d^{10} metal salt without any N-donor secondary ligand were also performed at a different condition, giving the compound **1**. However, when the auxiliary N-donor ligands of bpp, 4,4'-bpy, phen and 2,2'-bpy were introduced, six other perfect single crystals of complexes **2-7** were obtained. In addition, solvents including concentrated nitric acid, ethanol, $NaHCO_3$ and NaOH were used to adjust the pH value of the reaction, indicating the important role of pH value on the formation and the crystallization of coordination polymers. Actually, compounds **1−7** can be obtained only at a relative lower temperature below 120 °C.

Structural description

Crystal Structure of Complex 1. Compound **1** crystallizes in the triclinic system and *P*-1 space group. As shown in Fig. 1a, the asymmetric unit of **1** comprises one Zn (Ⅱ) ion, one $IDPA^{2-}$ ligand, one coordinated water and one free water molecule. The Zn (Ⅱ) center is five-coordinated and located in a distorted tetragonal pyramid geometry, which comprises of four oxygen atoms from H_2IDPA ligand and one oxygen atom from a water molecule. As listed in Table S1(ESI†), the Zn1–O4#1 bond distance is 2.5339(26) Å, which is somewhat longer than the other Zn1–O (O1, O2#2, O3#1, O1W; #1 x, y+1, z; #2 -x+1, -y, -z+2) bond distances in the range of 1.9537(19) to 1.987(2) Å, suggesting a nonnegligible interaction between them. However, the Zn1–O distance is comparable to other reported Zn(II) complexes.[18] Furthermore, it is worth noting that compound **1** exhibits one-dimensional (1D) chain structure constructed from binuclear Zn(II) clusters, which further extends into 2D supramolecular architecture *via* π-π interactions and hydrogen bonding interactions (Fig. 1b-c). As shown in Fig. 1c, the distances of intramolecular π-π interactions (two planes of C2⋯C3⋯C4⋯C6⋯C7⋯C8) are 3.6035(19) Å, which are in accordance with previous reports.[19] Due to the presence of a large number of coordinated water and free water molecules, there are abundant hydrogen bond donors (free water molecules) and hydrogen bond acceptors (deprotonated carboxyl groups and oxygen substitution) to construct a hydrogen bond network including intermolecular and intramolecular hydrogen bonding interactions (Table S3). To the best of our knowledge, it is still remain rare that a complicated supramolecular architecture assembled from simple chains *via* both π-π interactions and hydrogen bond interactions. As shown in Scheme 1a, there are two different coordination modes of $IDPA^{2-}$ ligands in **1**: μ_2-η^1:η^1-bridging and η^2-chelating. All the coordinated oxygen atoms are from the carboxy group while the oxygen atom of oxoisoindolin does not coordinate. On the basis of these connection modes, it forms a binuclear building unit thus obtaining an infinite 1D chain.

<void space for Scheme 2>
<void space for Fig. 1>

Crystal Structure of Complex 2. X-ray crystal structure analysis reveals that compound **2** belongs to a triclinic system with a space group *P*-1 and features a 2D layer structure completed by the polymetallic chains linked by bpp ligands. As shown in Fig. 2a, the asymmetric unit of **2** contains one independent Cd(II) ion, one independent $IDPA^{2-}$, one bpp and one free water molecule. Cd1 ion is seven-coordinated with a distorted monocapped octahedral geometry surrounded by five oxygen atoms from three $IDPA^{2-}$ ligands and two nitrogen atoms from two 4,4'-bpy ligands. The bond lengths of Cd−O (2.240-2.638 Å) and Cd−N (2.266-2.407 Å) are in line with those of reported compounds consisting of O−Cd−N segenments.[3c, 20] Every two Cd ions connect four H_2IDPA ligands and four bpp ligands, thus forming an infinite 1D polymetallic chain. The adjacent chains are associated by the bpp ligands connecting two Cd ions, giving a 2D sheet in the *ac* plane (Fig. 2b). It is worth noting that numerous intramolecular π-π interactions exist among the aromatic rings, as shown in Fig. 2c. The distances of intramolecular π-π interactions (two planes of N1···C9···C12···C11···C10, planes between C2···C3···C4···C6···C7···C8 and C11···C12···C13···-C14···C15··· C16) are 3.629(4) Å, 3.625(3) Å, respectively (PLATON),[21] which are in accordance with previous reports.[19c, 22] Furthermore, the two different coordination modes of $IDPA^{2-}$ ligands in **2** are η^2-chelating, μ_2-η^2:η^1-chelating and bridging (Scheme 2b). From a topological point view, the network topology of **2** was analyzed by considering the binuclear unit $[Cd_2(COO)_4]$ as a node, generating a single-node 4-connected ***sql*** tetragonal plane net with the Schläfli symbol of $\{4^4{\cdot}6^2\}$ (Fig. 2d-e).

<void space for Fig. 2>

Crystal Structure of Complex 3. The structure of **3** features a 3D framework with tubelike subunits containing open channel assembled by stacked metallomacrocycles. The single X-ray diffraction revealed that compound **3** crystallizes in the monoclinic system and $P2_1/n$ space group. There are one Cd(II) ion, one $IDPA^{2-}$ ligand and half a 4,4'-bpy molecule in the asymmetric unit of **3** (Fig. 3a). Cd1 ion is in a distorted monocapped octahedral geometry completed by five oxygen atoms from three carbanyl groups of $IDPA^{2-}$ ligand, one oxygen atom from the isoindolin-1-one group, one nitrogen atom from one 4,4'-bpy ligand. As shown in Fig. 3b, the basic building unit of **3** is a 17-membered metallomacrocycle, which is constructed from four Cd(II) ions bridged by two H_2IDPA ligands. Then the metallomacrocycles are extended by 4,4'-bpy linkers along the *b*-axis. Such kind of linkage in cooperation with the connection mode induces the formation of a relatively intricate 3D supramolecular architecture of **3** (Fig. 3c). In order to simplify the complicated connectivity of ligands and metal centers, the network topology of **3** was analyzed by considering the H_2IDPA ligand as a node, generating a binodal (4,5)-connected new topology with the Schläfli symbol of $\{4^2{\cdot}5^2{\cdot}6^2\}\{4^2{\cdot}5^3{\cdot}6^4{\cdot}7\}$ (Fig. 3d). In addition, coordination modes of $IDPA^{2-}$ ligands in **3** are the same as complex **2** except that the oxygen atom (O5) from the idl group of H_2IDPA ligand has been coordinated to Cd1 (Scheme 2c), which result in a torsion angle (15.757°) between benzene ring and idl substituent group (Fig. 3b).

<void space for Fig. 3>

Crystal Structure of Complex 4. Complex **4** was obtained only by employing $Zn(OAc)_2{\cdot}2H_2O$ (0.0219g, 0.1mmol) instead of $Cd(NO_3)_2{\cdot}4H_2O$ (0.0246g, 0.1mmol) for preparing **3**. Complex **4** crystallizes in the monoclinic space group *C*2/*c*. As can be found in Fig. 4a, the asymmetric unit of **4** contains one Zn(II) ion, one H_2IDPA ligand and half a 4,4'-bpy molecule. Zn1 ion locate in a slightly distorted octahedral coordination sphere formed by five carboxylic oxygen atoms of $IDPA^{2-}$ ligands and one nitrogen atom from one bridged 4,4'-bpy ligand. The carboxyl groups of one $IDPA^{2-}$ ligand exhibit η^2-chelating and μ_2-η^1:η^1-bridging coordination modes to assemble Zn(II) ions (Scheme 2a), inducing the formation of an infinite 2D polymetallic sheet (Fig. 4b). Then the adjacent planes are associated by the 4,4'-bpy ligands along the *a* axis, giving a novel 3D framework (Fig. 4c). In addition, complex **4** also exists intramolecular π-π interactions among the aromatic rings, as shown in Fig. S1a (ESI†). Furthermore, we select the H_2IDPA ligand and Zn(II) ion as nodes. From a topical point of view, although compound **4** has similar nodes as **3** (both **3** and **4** select the H_2IDPA ligand and metal ion as nodes**)**, it presents another distinct binodal (3,4)-connected new topology with the Schläfli symbol of $\{4{\cdot}6{\cdot}8\}\{4{\cdot}6^2{\cdot}8^3\}$ (Fig. 4d).

<void space for Fig. 4>

Crystal Structure of Complex 5. Single crystal X-ray diffraction analysis reveals that compound **5** features a 2D architecture completed by the polymetallic asymmetric unit with a monoclinic space group $P2_1/n$. There are four Zn(II) ions, four $IDPA^{2-}$ ligands, two phen ligands, two coordinated water molecules and two solvent water molecules in the asymmetric unit of **5**. As can be found in Fig. 5a, the coordination geometry of Zn1 ion locates in a distorted tetrahedral coordination geometry completed by four carboxylic oxygen atoms of four $IDPA^{2-}$ ligands. Both Zn2 and Zn3 ions are in a pyramidal coordination environment built from two nitrogen atoms of one phen ligand and three oxygen atoms of three $IDPA^{2-}$ ligands, one oxygen atom of coordinated water molecule and four oxygen atoms of four $IDPA^{2-}$ ligands, respectively. Zn4 is six-coordinated by one oxygen atom of one coordinated water molecule and two nitrogen atoms of phen ligand and three oxygen atoms of three $IDPA^{2-}$ ligands. The diagonal Zn1-Zn4 and Zn2-Zn3 separations are 3.6554 and 3.517 Å, respectively. As shown in Fig. 5b, the phen ligands are just chelated to Zn(II) ions and the adjacent tetranucleate blocks in a *ab* plane are connected by the $IDPA^{2-}$ ligands, forming a 2D sheet. Moreover, the 3D packing structure of **5** is stabilized by O–H···O and C–H···O hydrogen bonds, which originate from coordinated water and free water molecules, as well as those between hydrogen atoms of aromatic rings and oxygen atoms of the idl group (Table S3, ESI† and Fig. 5c). In addition, there are two different $IDPA^{2-}$ ligands, which have two different coordination modes: η^1 and μ_2-η^1:η^1- bridging (Scheme 2d-e). Every Zn(II) ion and their own symmetry-related ions are joined together by sharing two COO^- and one oxygen atom, thus forming a novel binuclear $[Zn_2(COO)_2O]$ building unit. Then the 2D sheet can be described as a uninodal 3-connected ***hcb*** net with the Schläfli symbol of $\{6^3\}$ (Fig. 5d). It is worth noting that a large apertures and voids in the structure are occupied by water molecules and calculations using PLATON show that the potential solvent area in compound **5** occupy 25.3% of the crystal volume (Fig. S1b, ESI†).[21]

<void space for Fig. 5>

Crystal Structure of Complex 6 and 7. Compound **6** was obtained similarly to **5** only by employing different solvent system while compound **7** was prepared similarly to **6** except that phen was replaced by 2,2'-bpy as secondary ligand. However, single X-ray diffraction analysis revealed that compounds **6** and **7** are isostructural and crystallize in a monoclinic space group $P2_1/c$. As a representative example, only the crystal structure of **6** is depicted here in details and the structure of **7** is shown in Fig. S2 (ESI†). As shown in Fig. 6a, the asymmetric unit of **6** consists of one Zn(II) ions, one IDPA^{2-} ligand, one phen ligands, one coordinated water molecule and one solvent water molecule. The octahedral coordination sphere around Zn1 ion is completed by three oxygen atoms from two IDPA^{2-} ligands, two nitrogen atoms from one phen ligand and one oxygen atom from one coordinated water molecule. As can be seen in Fig. 6b, the two carboxylic groups of IDPA^{2-} ligand as linkers assemble two Zn(II) ions and the two nitrogen atoms of 1,10-phen ligand just chelate to Zn(II) ions, forming a 1D infinite chain (Fig.6b). These chains are further packed into a 2D supramolecular network *via* intermolecular π-π interactions (face-face distance amounting to 3.535(4) A) and hydrogen bonds which are formed between the water molecules and the non-coordinated oxygen atoms of the carboxylic acid (Fig. 6c and Table S2-3, ESI†). In addition, the coordination mode of IDPA^{2-} ligand in **6** is the same as **5** (Scheme 2e) while compound **7** exhibits another different coordination mode: η^1 and η^1 (Scheme 2f).

<void space for Fig. 6>

The effect of secondary N-donor ligands and solvent system on the structures of 1–7

As can be seen in Scheme 2, six different coordination modes of H_2IDPA ligand exist in **1-7**. Compounds **1** is an infinite 1D chain obtained without any second ligand. In order to acquire more marvelous crystals, compounds **2-4** were synthesized under similar acidic conditions (pH=5.5) except different auxiliary ligands were used. They have different structures consisting of similar N-donor linkers for these three compounds. Compound **2** is 2D layer network with a novel 4-connected $\{4^4{\cdot}6^2\}$ topology, whereas compounds **3** and **4** present 3D structures with two new binodal (4,5)-connected $\{4^2{\cdot}5^2{\cdot}6^2\}\{4^2{\cdot}5^3{\cdot}6^4{\cdot}7\}$ and (3,4)-connected $\{4{\cdot}6{\cdot}8\}\{4{\cdot}6^2{\cdot}8^3\}$ topologies, respectively. For the four complexes **4–7**, the difference in their molecular structures reveals the significant effect of secondary N-donor ligands in tuning the molecular structures of coordination polymers. In particular, H_2IDPA ligand has been revealed to form isostructures of coordination polymers (complexes **6** and **7**) for Zinc metals with the help of phen and 2,2'-bpy as secondary ligand due to their similar coordination modes. From the viewpoint of solvent systems, compounds **5** and **6** are synthesized under the same mixtures with different solvent systems. When the pH value of a mixture containing H_2IDPA, Zn(II) salt, phen, DMF and water was adjusted to a closely neutral condition (pH=7.5), a 2D layer structure of **5** was obtained. Yet when the pH value of the above mixture of reactants was adjusted to the alkaline (pH =11) under similar reaction condition, a lower dimensional structure of complex **6** was prepared. The different solvent system affect the coordination modes of the H_2IDPA ligand and metal ions centers (two different coordination modes in **5** while only one coordination mode in **6**), which further result in different spatial structures of compounds **5** and **6**. Therefore, the secondary N-donor ligands and solvent system have significant effects on the structures of the resulting compounds.[1f, 9, 15c]

In addition, the effect of the bulky idl skeleton on structural assembly of **1–7** is also unnegligible. The extended π-conjugated system and the steric hindrance of the bulky idl ring not only affect the electron delocalization, but also result in π-π stacking interactions.[16c] As can be illustrated by above compounds **5-7**, it was because intermolecular π-π interactions and hydrogen bonds that made these low-dimensional coordination entities extend into higher-dimensional supramolecular networks.[15e, 22] 1,3-BDC is a typical aromatic carboxylic acid ligand, which has been widely applied to construct Zn/Cd (II) coordination polymers. However, when it was used to react with Zn(II) metal salts together with auxiliary 4,4'-bpy ligand, only a mononuclear 1D chain complex $[Zn(HBDC)_2(4,4'\text{-bpy})_2]_n$ was obtained.[23] In contrast, when the 1,3-BDC was replaced by H_2IDPA, a 3D CPs $[Zn(IDPA)(4,4'\text{-bpy})_{1/2}]_n$ was successfully constructed. This results indicate that although the available binding sites of 1,3-BDC and H_2IDPA are very similar, their coordination environment and the role for involving supramolecular interactions are different, which may be originate from the electronic nature and the bulky idl skeleton effect. Therefore, the present finding may provide an effective evidence for the preparation of new coordination architectures simply by changing the aromatic skeletons of different polycarboxyl systems from the viewpoint of ligand design.

Thermal Analysis and XRD Pattern

The thermal behavior for compounds **1−7** was investigated to reveal their thermal stability. The thermal curves are shown in Figure S3 (ESI†). For **1**, the weight loss of 8.99% in the range of 112-183 °C is attributed to the loss of two water molecules per unit cell (calc. 9.08%). Then the weight of complex **1** is stable until 443 °C. Subsequently, the weight dramatically diminish to 50.01% from 443-534 °C, corresponding to the loss of the organic framework. For **2**, the TG curve shows the water molecules are lost from 136 to 190 °C (obsd. 2.77%, calcd. 2.86%) and the decomposition temperature of the residual composition spans the range of 190 to 600 °C. The TG curves of complexes **3** and **4** are similar. The weight loss of **3** and **4** are not observed until 211 °C, 167 °C, respectively, owing to the decomposition of 4,4'-bpy (obsd.15.41%, calcd. 16.08% for **3**; obsd.17.17%, calcd. 17.80% for **4**). Then the residual composition decomposed from 375 to 503 °C for **3** and 326 to 650 °C for **4**. The TG curve of **5** shows the first weight loss of 3.95% occurs from 110 to 168 °C, corresponding to the loss of two coordinated water molecules and two free water molecules per unit cell (calcd. 3.84%). Subsequently, the weight continues to diminish from 168 to 490°C owing to the decomposition of two phen molecules (obsd.20.03%, calcd. 21.14%). Because complexes **6** and **7** are isostructural, they present similar thermal stability and are stable to about 70 °C. The continuous weight loss from 70 to 160 °C correspond to the loss of two water molecules (obsd. 6.95%, calcd. 6.24% for **6** and obsd. 6.73%, calcd. 6.51% for **7**). Upon heating beyond 160 °C, the organic ligands begin decomposing, leading to a collapse of the framework.

In addition, the purity of the complexes **1−7** was also supported by the powder X-ray diffraction analysis result (Fig. S4, ESI†). The peaker positions of the experimental patterns are in good agreement with the simulated ones, which clearly indicate good purity and homogeneity of the compounds.

Luminescent Property of Complexes 1−7

Taking into account the excellent luminescent properties of d^{10} complexes, the luminescence spectra of **1−7** have been recorded in the solid state at room temperature. In order to understand these emission bands, we have also investigated the luminescent properties of the free ligands including 1,3-BDC, H_2IDPA and four auxiliary N-donor ligands. As shown in Fig. 7a, the emission bands are 327 nm and 345 nm (λ_{ex}=265 nm) for 1,3-BDC, 439 nm (λ_{ex}=365 nm) for H_2IDPA, 402 nm (λ_{ex}=320 nm) for 4,4'-bpy, 388 nm (λ_{ex}=325 nm) for 2,2'-bpy, 364 nm, 380 nm and 400 nm (λ_{ex}= 248 nm) for 1,10-phen, respectively, which can be probably assigned to π to π* or n orbital transitions.[24] Compared to the 1,3-BDC, H_2IDPA exhibits a large red shit (100 nm) as well as in other N-donor ligands, which may be tentatively assigned to extended π-conjugated system that decreases the molecular band gap. For the complexes **1-7**, the strong blue emission bands and excitation wavelengths are listed in Table 2. Despite the use of different secondary ligands, the luminescent intensity of **1-7** have been increased and emission spectras are all blue shifted compared to the free ligand. The emissions spectra may be a mixture of characters of intraligand and LLCT, and the observed blue shift of the emission maximum was considered to mainly originate from the increasing of rigidity by the metal coordination, and H-aggregation of π-systems as well.[3b, 15c, 25] Notably, although both Zn(II) compounds **5** and **6** are formed by H_2IDPA and phen ligands, they show different fluorescence properties that compound **5** has another green emission band at 543nm. This may be a result of their different formations and structure (2D coordination polymers for **4** and 1D coordination polymers for **5**).[9, 26] Moreover, the different locations and profiles of their emission peaks of **1–7** are probably due to different metal centers, different ancillary ligands and coordination modes of ligand as well as weak interactions in the network lattice, affecting the rigidity of the whole network and promoting the energy transfer involved in the luminescence.[1d, 3d, 27]

<void space for Table 2>

<void space for Fig. 7>

In order to further study the luminescence properties, the corresponding QY and decay lifetimes for H_2IDPA ligand and compounds **1-7** were obtained and listed in Table 2. The QY of compounds **3** and **4** (2.23%, 3.41%, respectively) with 3D network regulated by 4,4'-bpy are lower than H_2IDPA ligand (QY_{H_2IDPA}=4.41%). However, when the low-dimensional compounds **2** and **7** were synthesized with the help of other auxiliary ligands, their QY reach up to 39.80% and 28.14%, respectively, which are much higher than the free ligands (QY_{bpp}<1%, $QY_{2,2'\text{-}bpy}$<1%) and compound **1** (QY_1=6.32%). The high QY of compounds **2** and **7** are probably attributed to the immobilization of H_2IDPA ligand as it is strongly coordinated to metal ions that effectively increase the rigidity of the ligands, and to the low-dimensional structure with π-conjugated system decreases the molecular band gap.[4b, 28] Furthermore, the H_2IDPA ligands fixed in the MOFs with metal ions and auxiliary ligands have longer intermolecular separations and, as a result, can increase photoluminescence QY due to decreased self-quenching.[28c] In addition, the luminescence decay curves can be fitted by an exponential function as $I(t)= A\exp(-t/\tau)$. The longest luminescent lifetimes of these compounds is only 59 ns, which is much shorter than the ones resulting from a triplet state (>10^{-3} s), so the emissions should arise from a singlet state.[9, 29] The QY and decay curves of a representative compounds **2** and H_2IDPA ligand are shown in Fig. 8 (Fig. 8a-b for **2**; Fig. 8c-d for H_2IDPA; Fig. S5-8 for bpp, 2,2'-bpy, complexes **1** and **3-7**, ESI†). The photoluminescence properties of these compounds indicate that they could be potentially used as luminescent materials.

<void space for Fig. 8>

Conclusions

In conclusion, we introduced a new π-conjugated carboxylate ligand with coplanar substituents and their Zn/Cd (II) complexes with the help of auxiliary N-donor ligands including bpp, phen, 4,4'-bpy and 2,2'-bpy. Complexes **1-7** display strong luminescence properties and may become potential candidates for blue luminescent materials. The diverse structures of the compounds ranging from 1D chain to 3D supramolecular network give rise to different luminescent intensity, especially that the QY of compound **2** reaches at 39.80%. In summary, the research demonstrates an improved effect of π-conjugated system on luminescence properties, providing a guiding strategy when synthesizing MOFs with attractive properties.

Acknowledgements

This work was supported by the "Strategic Priority Research Program" of the Chinese Academy of Sciences (XDA07070200, XDA09030102), National Key Technology R&D Program (2012BAE06B08), the Chinese Academy of Sciences (KJCX2-YW-H30), the Science Foundation of Fujian Province (2006l2005) and Fujian industrial guide project (2015H0053).

References

1 (a) L.-B. Sun, A.-G. Li, X.-D. Liu, X.-Q. Liu, D. Feng, W. Lu, D. Yuan and H.-C. Zhou, *J. Mater. Chem. A*, 2015, **3**, 3252; (b) L. Liu, Z. B. Han, S. M. Wang, D. Q. Yuan and S. W. Ng, *Inorg. Chem.*, 2015, **54**, 3719; (c) Q.-R. Fang, G.-S. Zhu, Z. Jin, Y.-Y. Ji, J.-W. Ye, M. Xue, H. Yang, Y. Wang and S.-L. Qiu, *Angew. Chem. Int. Edit.*, 2007, **119**, 6758; (d) X. Zhang, Y. Y. Huang, Q. P. Lin, J. Zhang and Y. G. Yao, *Dalton trans.*, 2013, **42**, 2294; (e) H. Reinsch, M. A. van der Veen, B. Gil, B. Marszalek, T. Verbiest, D. de Vos and N. Stock, *Chem. Mater.*, 2013, **25**, 17; (f) Z. Ju and D. Yuan, *CrystEngComm*, 2013, **15**, 9513; (g) M.

Sasaki, Y. Sato, Y. Tsuboi, S. Inagaki and Y. Kubota, *ACS Catal.*, 2014, **4**, 2653; (h) Y.-X. Tan, Y.-P. He and J. Zhang, *Chem. Mater.*, 2012, **24**, 4711.

2 (a) T. K. Prasad, D. H. Hong and M. P. Suh, *Chem.-Eur. J.*, 2010, **16**, 14043; (b) H.-R. Fu, Z.-X. Xu and J. Zhang, *Chem. Mater.*, 2015, **27**, 205; (c) N. Stock and S. Biswas, *Chem. Rev.*, 2012, **112**, 933; (d) Y.-F. Yue, J. Liang, E.-Q. Gao, C.-J. Fang, Z.-G. Yan and C.-H. Yan, *Inorg. Chem.*, 2008, **47**, 6115.

3 (a) Y. Mikata, Y. Sato, S. Takeuchi, Y. Kuroda, H. Konno and S. Iwatsuki, *Dalton Trans.*, 2013, **42**, 9688; (b) S.-Q. Zhang, F.-L. Jiang, M.-Y. Wu, J. Ma, Y. Bu and M.-C. Hong, *Cryst. Growth Des.*, 2012, **12**, 1452; (c) W. Yang, C. Wang, Q. Ma, C. Liu, H. Wang and J. Jiang, *CrystEngComm*, 2014, **16**, 4554; (d) Z. Chang, A.-S. Zhang, T.-L. Hu and X.-H. Bu, *Cryst. Growth Des.*, 2009, **9**, 4840.

4 (a) Y. Hong, J. W. Y. Lam and B. Z. Tang, *Chem. Soc. Rev.*, 2011, **40**, 5361; (b) M. Zhang, G. Feng, Z. Song, Y. P. Zhou, H. Y. Chao, D. Yuan, T. T. Tan, Z. Guo, Z. Hu, B. Z. Tang, B. Liu and D. Zhao, *J. Am. Chem. Soc.*, 2014, **136**, 7241.

5 (a) R. Hu, N. L. Leung and B. Z. Tang, *Chem. Soc. Rev.*, 2014, **43**, 4494; (b) N. B. Shustova, T. C. Ong, A. F. Cozzolino, V. K. Michaelis, R. G. Griffin and M. Dinca, *J. Am. Chem. Soc.*, 2012, **134**, 15061; (c) Y. Hong, J. W. Lam and B. Z. Tang, *Chem. Commun.*, 2009, **29**, 4332; (d) N. B. Shustova, A. F. Cozzolino and M. Dinca, *J. Am. Chem. Soc.*, 2012, **134**, 19596.

6 (a) Z. P. Wang, J. Y. Wang, J. R. Li, M. L. Feng, G. D. Zou and X. Y. Huang, *Chem. Commun.*, 2015, **51**, 3094; (b) A. J. LEES, *Chem. Rev.*, 1987, **87**, 711; (c) J. V. Houten and R. J. Watts, *J. Am. Chem. Soc.*, 1976, **98**, 4853.

7 (a) Andrzej M. Kłonkowski, S. Lis, M. Pietraszkiewicz, Z. Hnatejko, K. Czarnobaj and M. Elbanowski, *Chem. Mater.*, 2003, **15**, 656; (b) S. J. A. Pope, A. M. Kenwright, S. L. Heath and S. Faulkner, *Chem. Commun.*, 2003, **13**, 1550.

8 H.-S. Shou, J.-P. Ye and Q. Yu, *J. Lumin.*, 1998, **42**, 29.

9 D.-L. Yang, X. Zhang, Y.-G. Yao and J. Zhang, *CrystEngComm*, 2014, **16**, 8047.

10 Y. Sun, N. Ross, S.-B. Zhao, K. Huszarik, W.-L. Jia, R.-Y. Wang, D. Macartney and S. Wang, *J. Am. Chem. Soc.*, 2007, **129**, 7510.

11 (a) B. Moulton, J. Lu, R. Hajndl, S. Hariharan and M. J. Zaworotko, *Angew. Chem. Int. Edit.*, 2002, **41**, 2821; (b) D. Zhao, D. Yuan, A. Yakovenko and H.-C. Zhou, *Chem. Commun.*, 2010, **46**, 4196; (c) P. Ren, W. Shi and P. Cheng, *Cryst. Growth Des.*, 2008, **8**, 1097.

12 (a) J. Zhang, Y.-B. Chen, S.-M. Chen, Z.-J. Li, J.-K. Cheng and Y.-G. Yao, *Inorg. Chem.*, 2006, **45**, 3161; (b) L. Xu, E.-Y. Choib and Y.-U. Kwon, *Inorg. Chem. Commun.*, 2008, **11**, 1190.

13 (a) J. Gao, N. Wang, X. Xiong, C. Chen, W. Xie, X. Ran, Y. Long, S. Yue and Y. Liu, *CrystEngComm*, 2013, **15**, 3261; (b) M. A. Braverman and R. L. LaDuca, *CrystEngComm*, 2008, **10**, 117; (c) J.-D. Lin, J.-W. Cheng and S.-W. Du, *Cryst. Growth Des.*, 2008, **8**, 3345.

14 (a) Z.-J. Lin, T.-F. Liu, B. Xu, L.-W. Han, Y.-B. Huang and R. Cao, *CrystEngComm*, 2011, **13**, 3321; (b) Z. Chang, D. S. Zhang, Q. Chen, R. F. Li, T. L. Hu and X. H. Bu, *Inorg. Chem.*, 2011, **50**, 7555; (c) J. Ma, F. L. Jiang, L. Chen, M. Y. Wu, S. Q. Zhang, D. Han, R. Feng and M. C. Hong, *Cryst. Growth Des.*, 2011, **11**, 3273.

15 (a) T. R. Cook, Y.-R. Zheng and P. J. Stang, *Chem. Rev.*, 2013, **113**, 734; (b) M. Du, C.-P. Li, C.-S. Liu and S.-M. Fang, *Coord. Chem. Rev.*, 2013, **257**, 1282; (c) W. Yang, C. Wang, Q. Ma, X. Feng, H. Wang and J. Jiang, *Cryst. Growth Des.*, 2013, **13**, 4695; (d) M.-M. Dong, L.-L. He, Y.-J. Fan, S.-Q. Zang, H.-W. Hou and T. C. W. Mak, *Cryst. Growth Des.*, 2013, **13**, 3353; (e) J. Chen, G.-P. Yang, W.-H. Huang, L.-Y. Pang, C.-P. Zhang, Y.-Y. Wang and Q.-Z. Shi, *Inorg. Chim. Acta*, 2013, **400**, 7.

16 (a) Z. Zhang, L. Wojtas and M. J. Zaworotko, *Cryst. Growth Des.*, 2011, **11**, 1441; (b) C. Liu, W. Li, D. Du, D. Zhu and L. Xu, *Z. Anorg. Allg. Chem.*, 2011, **637**, 1253; (c) S. M. Fang, M. Hu, Q. Zhang, M. Du and C. S. Liu, *Dalton Trans.*, 2011, **40**, 4527; (d) D. Singh, P. K. Bhattacharyya and J. B. Baruah, *Cryst. Growth Des.*, 2010, **10**, 348.

17G. M. Sheldrick, *SHELXL-97, Program for Solution of Crystal Structures,University of Göttingen, Göttingen, Germany,*, 1997.

18 (a) J.-J. Cheng, Y.-T. Chang, C.-J. Wu, Y.-F. Hsu, C.-H. Lin, D. M. Proserpio and J.-D. Chen, *CrystEngComm*, 2012, **14**, 537; (b) Y.-L. Wei, J.-B. Li, W.-C. Song and S.-Q. Zang, *Inorg. Chem. Commun.*, 2012, **15**, 16; (c) Y. Zhao, L.-L. He, H. Xu, X.-Y. Li and S.-Q. Zang, *Inorg. Chim. Acta*, 2013, **404**, 201.

19 (a) C. Janiak, *J. Chem. Soc. Dalton Trans.*, 2000, **21**, 3885; (b) T. Yang, J. J. An, X. Wang, D. Y. Wu, W. Chen and J. S. Fossey, *Phys. Chem. Chem. Phys.*, 2012, **14**, 10747; (c) J. Zukerman-Schpector and E. R. T. Tiekink, *CrystEngComm*, 2014, **16**, 6398.

20 (a) C.-X. Meng, D.-S. Li, J. Zhao, F. Fu, X.-N. Zhang, L. Tang and Y.-Y. Wang, *Inorg. Chem. Commun.*, 2009, **12**, 793; (b) W.-G. Lu, C.-Y. Su, T.-B. Lu, L. Jiang and J.-M. Chen, *J. Am. Chem. Soc.*, 2006, **128**, 34; (c) W. G. Lu, J. Z. Gu, L. Jiang, M. Y. Tan and T. B. Lu, *Cryst. Growth Des.*, 2008, **8**, 192.

21 A. L. Spek, *J. Appl. Crystallogr.*, 2003, **36**, 7.

22 H. Wang, K. Wang, D. Sun, Z.-H. Ni and J. Jiang, *CrystEngComm*, 2011, **13**, 279.

23 E. Tang, Y.-M.Dai and S. Lin, *Acta Crystallogr., Sect. C: Cryst. Struct. Commun.*, 2004, **60**, 433.

24 Y.-Q. Lan, S.-L. Li, Y.-M. Fu, D.-Y. Du, H.-Y. Zang, K.-Z. Shao, Z.-M. Su and Q. Fu, *Cryst. Growth Des.*, 2009, **9**, 1353.

25 X.-Y. Chen, A. M. Plonka, D. Banerjee and J. B. Parise, *Cryst. Growth Des.*, 2013, **13**, 326.

26 D.-L. Yang, X. Zhang, J.-X. Yang, Y.-G. Yao and J. Zhang, *Inorg. Chim. Acta*, 2014, **423**, 62.

27 (a) Y. Cui, Y. Yue, G. Qian and B. Chen, *Chem. Rev.*, 2012, **112**, 1126; (b) X.-L. Chen, B. Zhang, H.-M. Hu, F. Fu, X.-L. Wu, T. Qin, M.-L. Yang, G.-L. Xue and J.-W. Wang, *Cryst. Growth Des.*, 2008, **8**, 3706; (c) A. H. Shelton, I. V. Sazanovich, J. A. Weinstein and M. D. Ward, *Chem. Commun.*, 2012, **48**, 2749.

28 (a) Y.-B. Chen, J. Zhang, J.-K. Cheng, Y. Kang, Z.-J. Li and Y.-G. Yao, *Inorg. Chem. Commun.*, 2004, **7**, 1139; (b) L.-N. Zhu, L. Z. Zhang, W.-Z. Wang, D.-Z. Liao, P. Cheng, Z.-H. Jiang and S.-P. Yan, *Inorg. Chem. Commun.*, 2002, **5**, 1017; (c) Z. Wei, Z. Y. Gu, R. K. Arvapally, Y. P. Chen, R. N. McDougald, Jr., J. F. Ivy, A. A. Yakovenko, D. Feng, M. A. Omary and H. C. Zhou, *J. Am. Chem. Soc.*, 2014, **136**, 8269.

29 (a) Y.-Y. Liu, J.-F. Ma, J. Yang, J.-C. Ma and Z.-M. Su, *CrystEngComm*, 2008, **10**, 894; (b) J.-F. Ma, J. Yang, S.-L. Li and S.-Y. Song, *Cryst. Growth Des.*, 2005, **5**, 807.

Table 1 Crystallographic data and structure refinement of complexes **1-7.**

Complex	**1**	**2**	**3**	**4**	**5**	**6**	**7**
Formula	$C_{16}H_{13}ZnNO_7$	$C_{29}H_{25}CdN_3O_6$	$C_{21}H_{13}CdN_2O_5$	$C_{21}H_{13}ZnN_2O_5$	$C_{88}H_{60}Zn_4N_8O_{24}$	$C_{28}H_{21}ZnN_3O_7$	$C_{26}H_{21}N_3ZnO_7$
FW	396.66	623.91	485.74	438.72	1874.97	576.87	552.85
Crystal system	Triclinic	Triclinic	Monoclinic	Monoclinic	Monoclinic	Monoclinic	Monoclinic
Space group	*P*-1	*P*-1	$P2_1/n$	$C2/c$	$P2_1/n$	$P2_1/c$	$P2_1/c$
a (Å)	7.8996(5)	10.1604(6)	9.9520(3)	24.0555(9)	22.120(6)	9.5144(5)	8.6783(4)
b (Å)	9.7188(4)	11.2134(6)	12.9516(4)	7.7920(3)	17.647(4)	18.7601(7)	18.8256(7)
c (Å)	10.8839(7)	12.1942(7)	13.4675(5)	18.1219(6)	25.391(6)	13.7258(5)	14.1402(6)
α (°)	97.916(4)	102.647(5)	90	90	90	90	90
β (°)	95.921(6)	95.448(4)	104.847(4)	100.783(3)	97.171(4)	92.244(4)	91.928(4)
γ (°)	113.064(5)	107.156(5)	90	90	90	90	90
V (Å^3)	750.09(7)	1276.19(13)	1677.93(10)	3336.8(2)	9834(4)	2448.05(18)	2308.84(17)
Z	2	2	4	8	4	4	4
D_{calcd} (g·cm^{-1})	1.756	1.618	1.923	1.747	1.264	1.565	1.590
μ (mm^{-1})	1.680	0.906	1.324	1.513	1.034	1.059	1.119
F(000)	404.0	628	964	1784	3808	1184	1136
R_{int} I > 2θ	0.0348	0.0477	0.0326	0.0320	0.0791	0.0306	0.0348
R_{w2} I > 2θ	0.0757	0.1242	0.0691	0.0709	0.2501	0.0715	0.0732
R_1^{a}	0.0435	0.0551	0.0408	0.0435	0.0990	0.0344	0.0495
R_{w2}^{b}	0.0812	0.1309	0.0724	0.0766	0.2777	0.0741	0.0809
S	1.051	1.075	1.114	1.078	1.054	1.049	1.060

$^aR_1=\Sigma||F_o| - |F_c||/\Sigma|F_o|$. $^bR_{w2}=[\Sigma w(F_o^2 - F_c^2)^2/\Sigma w(F_o^2)^2]^{1/2}$

Table 2 The luminescence properties of the ligand (H_2IDPA) and compounds **1-7**.

Sample	**Excitation wavelength (nm)**	**Maximum emission Wavelength (nm)**	**Decay (ns)**	**Quantum yield (%)**
H_2IDPA	365	439	38	4.41
1	340	420	27	6.32
2	365	423	28	39.80
3	340	423	30	2.23
4	340	418	24	3.41
5	340	435	36	8.21
6	365	435	33	14.68
7	340	435	59	28.14

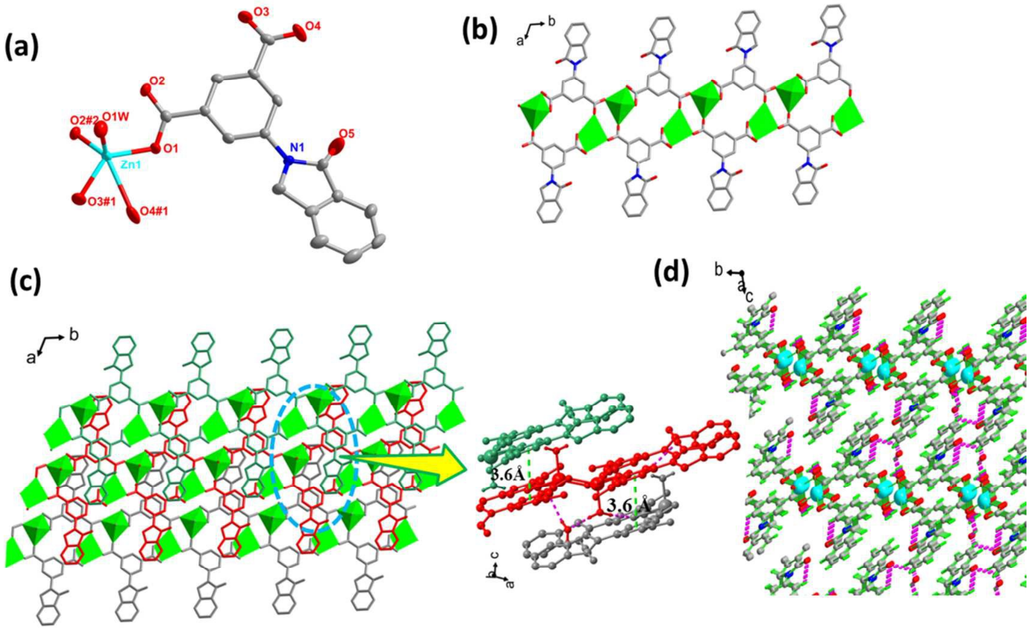

Fig. 1 (a) Coordination environments of Zn (II) ion with 40% thermal ellipsoids. (b) An infinite 1D chain composed of binuclear subunits view along the crystallographic c-axis. (c) 2D supramolecular network *via* intermolecular π-π interactions (green bonds) and hydrogen bonds (pink bonds) along the *ab* plane. All hydrogen atoms and water molecules have been omitted for clarity. (d) The packing diagram of **1**. (Symmetry codes: #1 x, y+1, z; #2 -x+1, -y, -z+2).

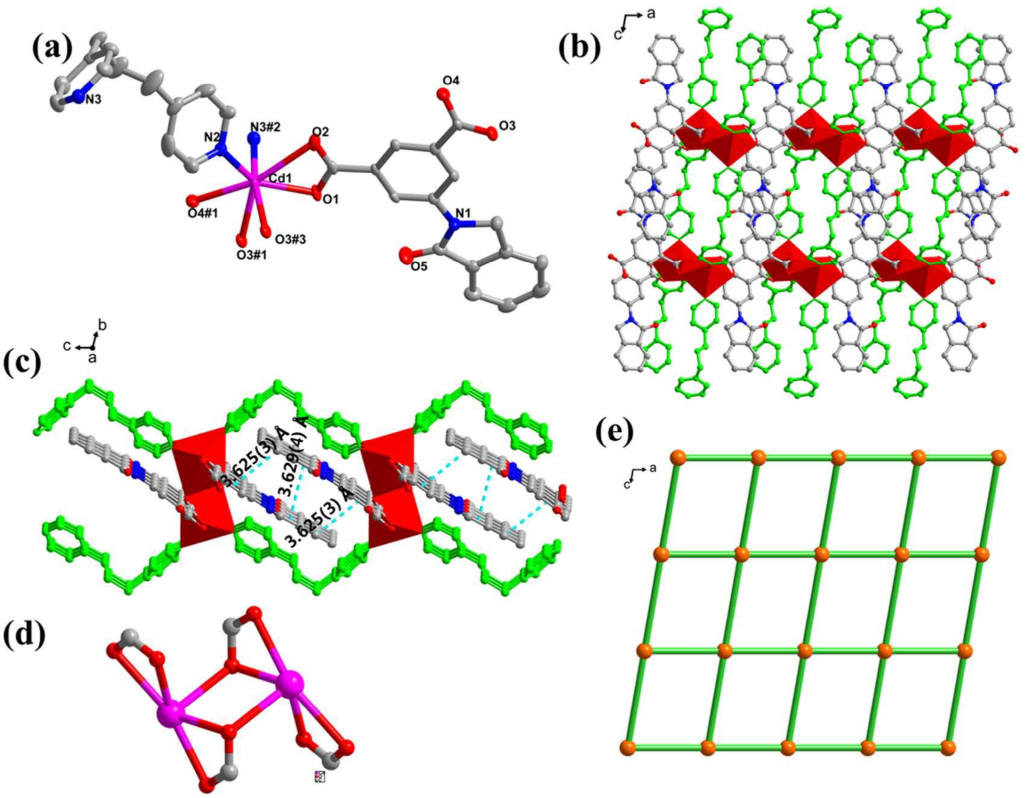

Fig. 2 (a) Coordination environments of Cd(II) ion with 40% thermal ellipsoids. (b) View of the 2D layer along *c*-axis with hydrogen and guest molecules omitted for clarity. (c) View of the 2D layer along *a*-axis with π-π interactions existing among the aromatic rings. (d) Binuclear [$Cd_2(COO)_4$] building unit. (e) Schematic representation of the 4-connected ***sql*** topology of **2**. (Symmetry codes: #1 x-1, y, z; #2 x, y, z-1; #3 -x+2, -y+1, -z+1).

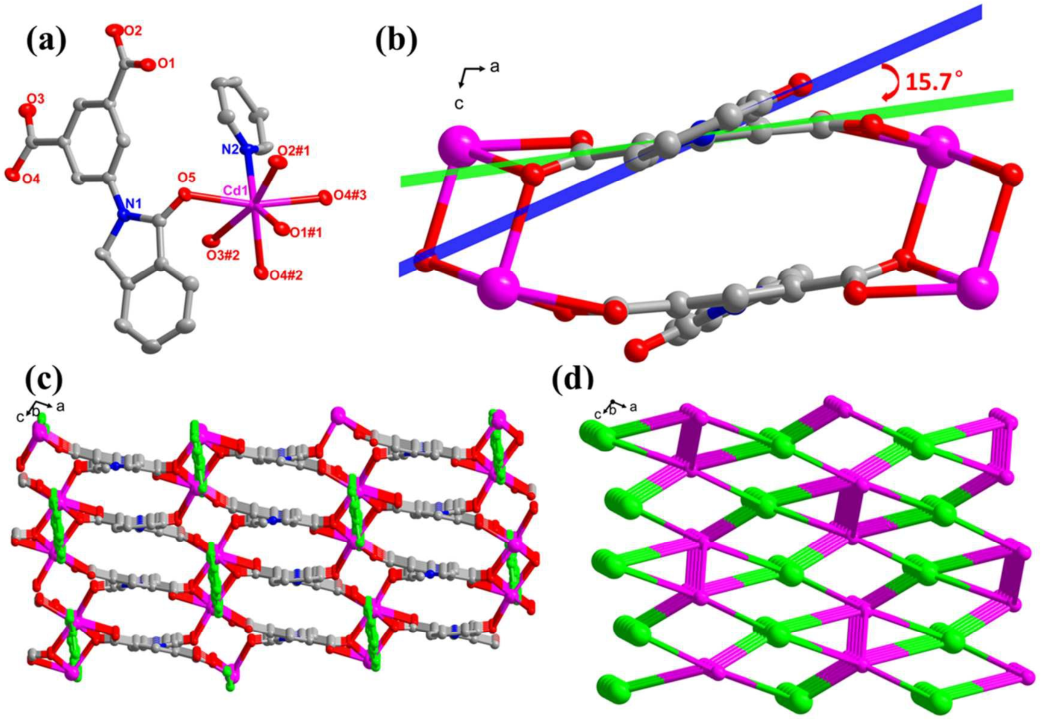

Fig. 3 (a) Coordination environments of Cd(II) ion with 40% thermal ellipsoids. (b) A 17-membered metallomacrocycle in **3**. (c) 3D structure of **3** viewed along the *b*-axis. (d) Schematic representation of a binodal (4,5)-connected topology of **3**. (Symmetry codes: #1 -x+3/2, y-1/2, -z+1/2; #2 -x+1/2, y-1/2, -z+1/2; #3 x+1/2, -y+1/2, z-1/2).

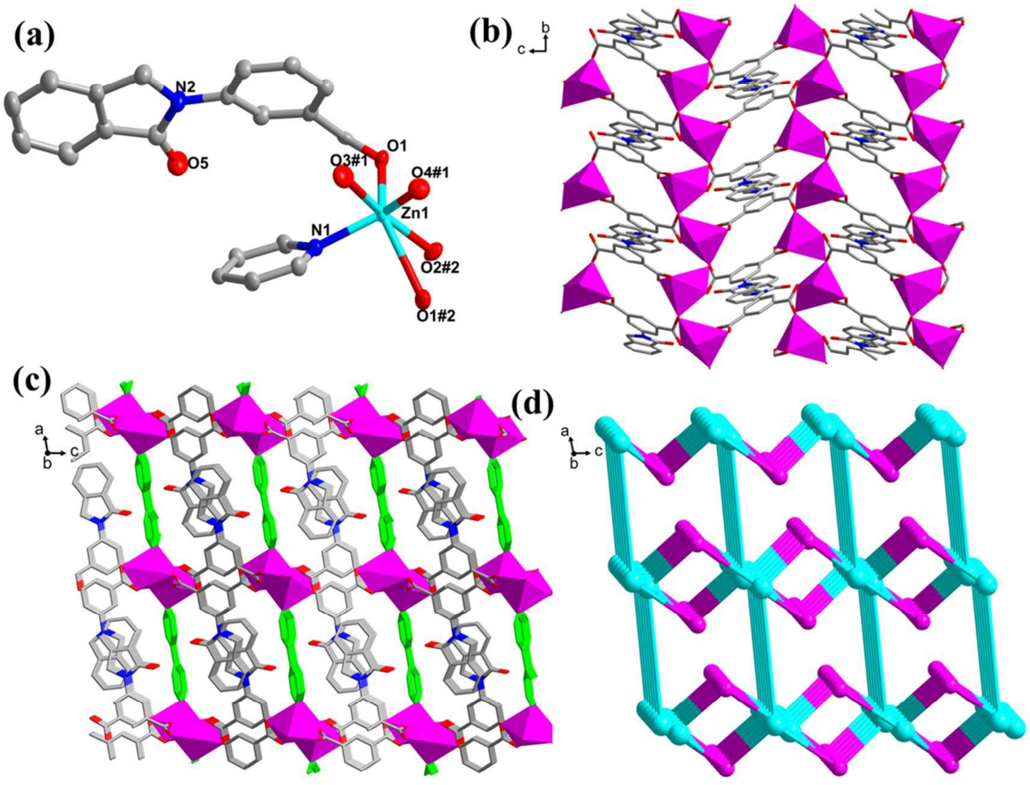

Fig. 4 (a) Coordination environments of Zn(II) ion with 40% thermal ellipsoids. (b) An infinite 2D polymetallic sheet. (c) 3D structure of **4** viewed along the *b*-axis. (d) Schematic representation of a binodal (3,4)-connected topology of **4**. (Symmetry codes: #1 -x+1/2, -y-1/2, -z+1; #2 -x+1/2, y-1/2, -z+1/2).

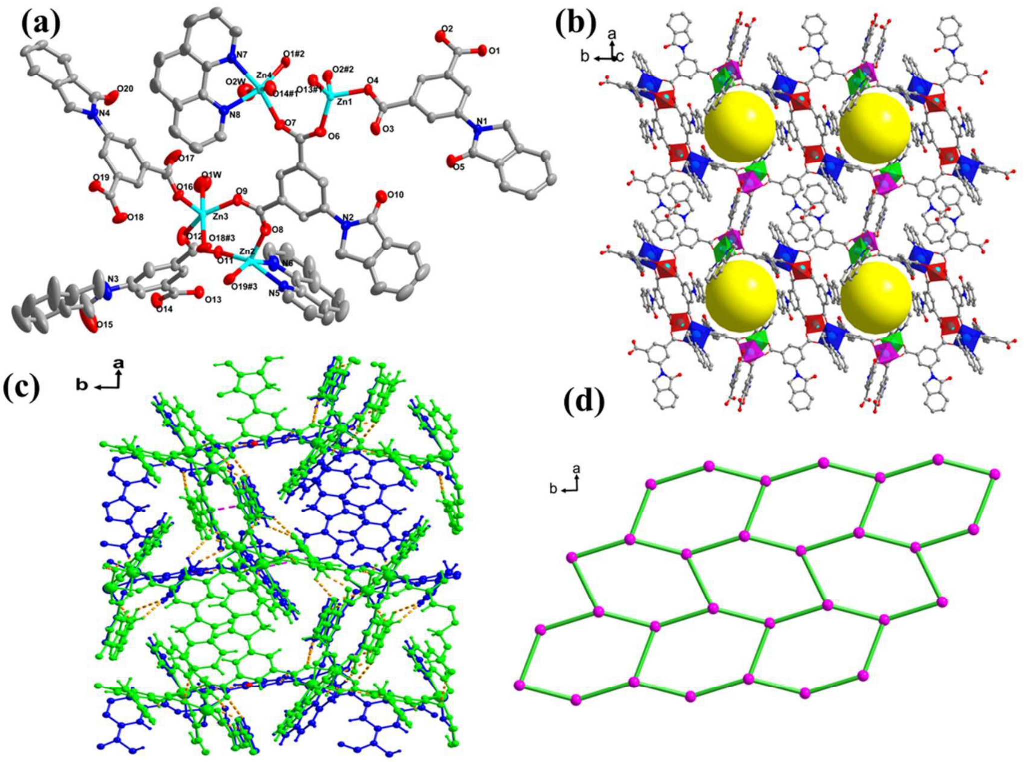

Fig. 5 (a) Coordination environments of Zn(II) ion with 40% thermal ellipsoids. (b) View of the 2D layer along *c*-axis with hydrogen and guest molecules omitted for clarity. (c) 3D packing structure of **5** with hydrogen bonds. (d) Schematic representation of the 3-connected ***hcb*** topology of **5**. (Symmetry codes: #1 x, y-1, z; #2 -x, -y, -z+1; #3 -x+1, -y+1, -z+1).

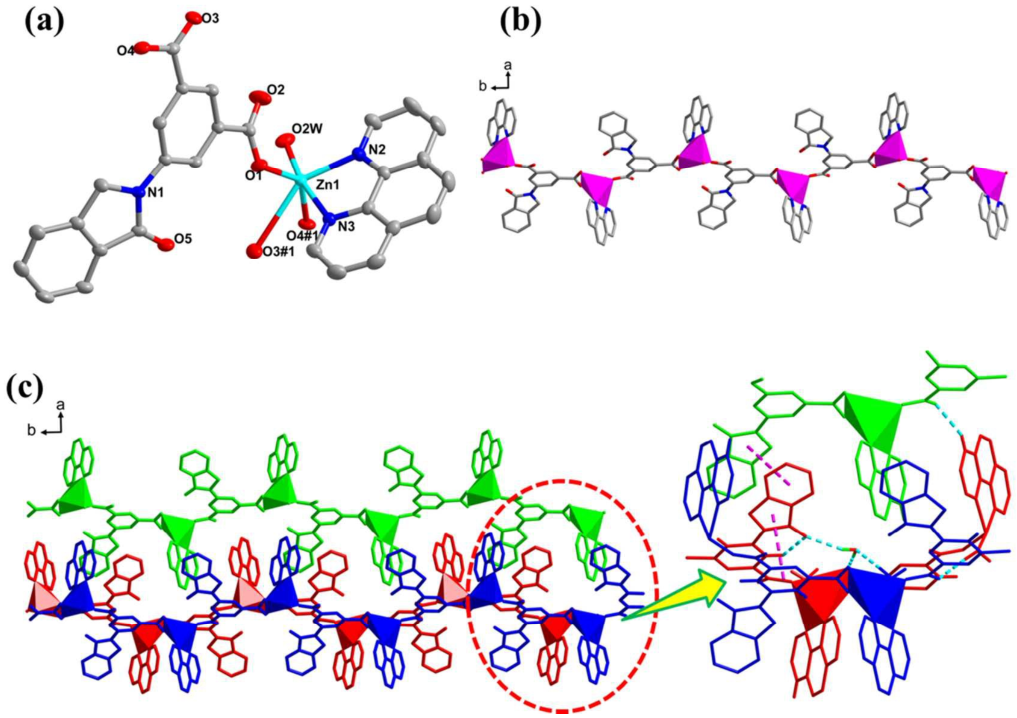

Fig. 6 (a) Coordination environments of Zn (II) ion with 40% thermal ellipsoids. (b) An infinite 1D chain of **6** viewed along the crystallographic *c*-axis. (c) 2D supramolecular network via intermolecular π-π interactions and hydrogen bonds. (Symmetry codes: #1 -x+1, y+1/2, -z+3/2).

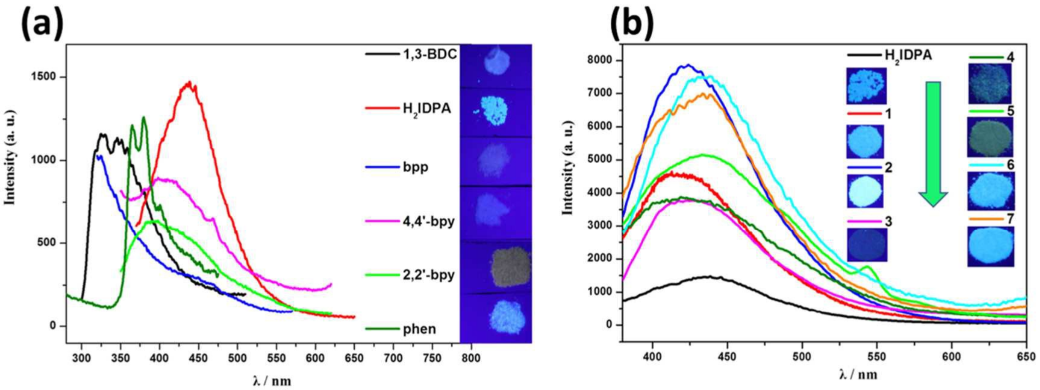

Fig. 7 The emission spectra of organic ligands and **1-7** in the solid state at room temperature. The insert photos were taken under UV lamp with excitation wavelength of 365nm.

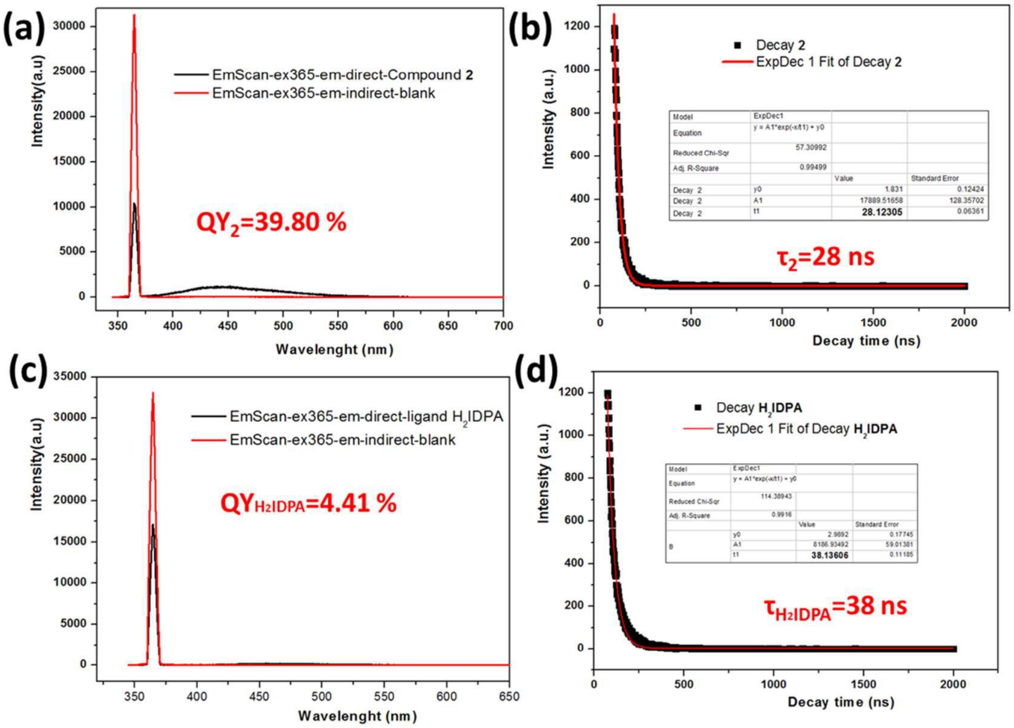

Model	ExpDec1		
Equation	y = A1*exp(-x/t1) + y0		
Reduced Chi-Sqr	57.30992		
Adj. R-Square	0.99499		
		Value	Standard Error
Decay 2	y0	1.831	0.12424
Decay 2	A1	17889.51658	128.35702
Decay 2	t1	**28.12305**	0.06361

Model	ExpDec1		
Equation	y = A1*exp(-x/t1) + y0		
Reduced Chi-Sqr	114.38943		
Adj. R-Square	0.9916		
		Value	Standard Error
B	y0	2.9892	0.17745
	A1	8186.93492	59.01381
	t1	**38.13606**	0.11185

Fig. 8 The QY and Decay curves of compound **2** (a, b) and H_2IDPA ligand (c, d).

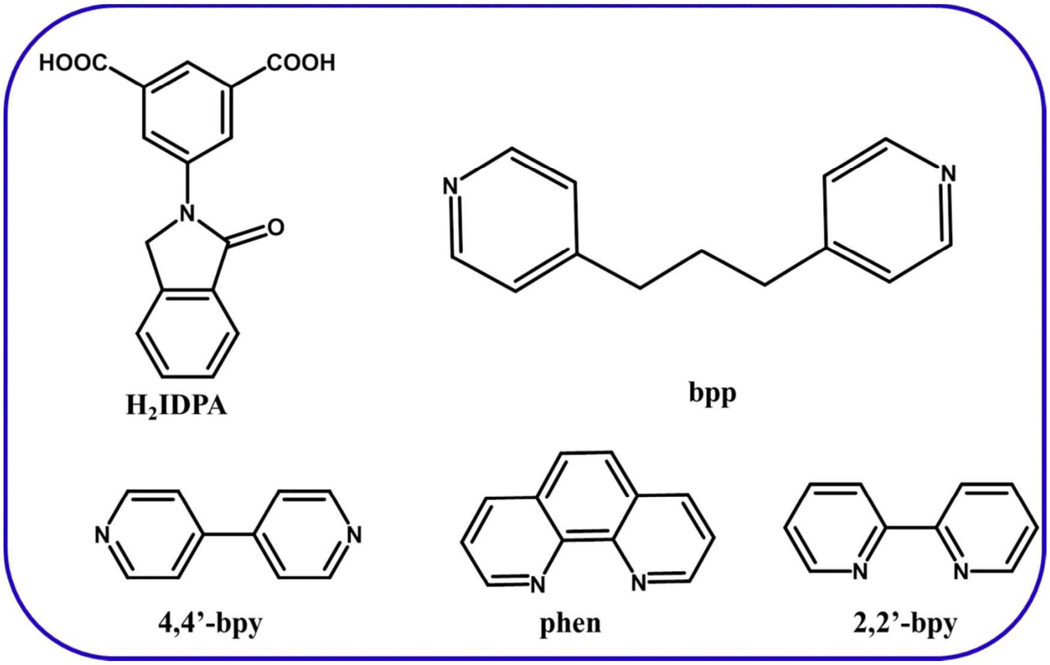

Scheme 1 Schematic molecular structures of H_2IDPA and N-donor ligands.

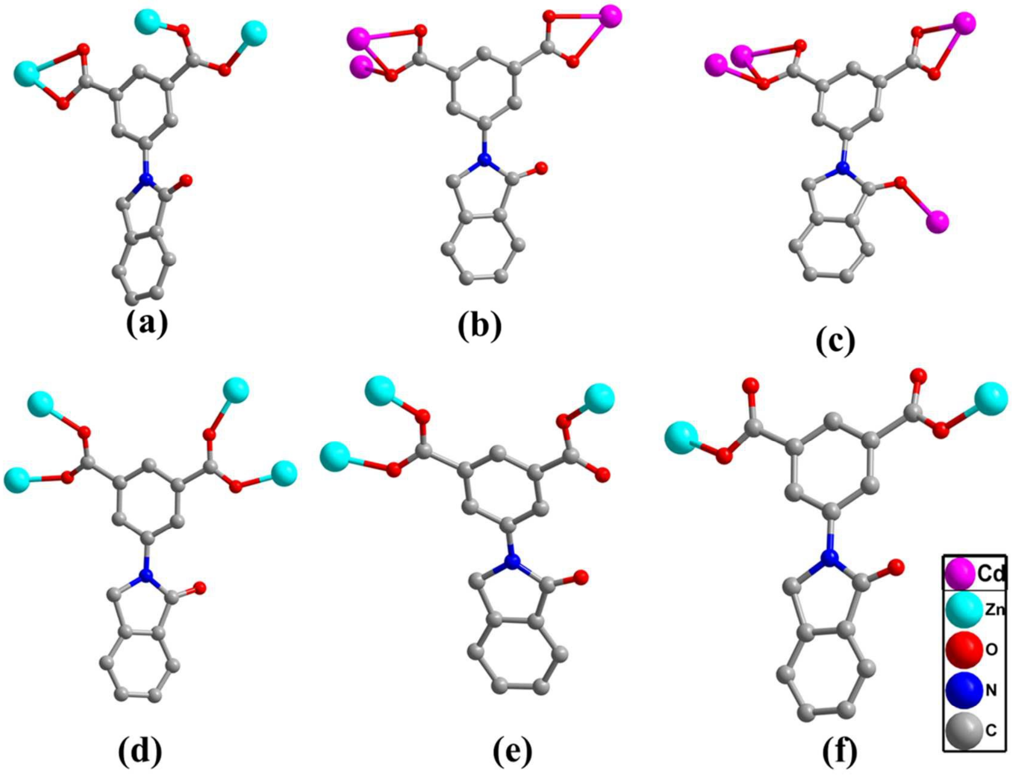

Scheme 2 The coordination modes of the H_2IDPA ligand in compounds **1–7** [(a) for **1** and **4**;(b) for **2**;(c) for **3**; (d-e) for **5**; (e) for **6**, (f) for **7**].

Graphical Abstract

Aggregation-induced emission (AIE) has been identified and studied based on a bulky π-conjugated ligand (H_2IDPA) with Zn/Cd^{II} metals.